

Performance Evaluation of Built-In Small LF Antennas inside a Metal Case

Kazuaki ABE^{†,††a)} and Jun-ichi TAKADA^{††}, *Members*

SUMMARY This paper describes a method for evaluating the performance of a small magnetic core loop antenna used for radio controlled watches. Recently, amorphous metal core loop antennas are used as built-in small antennas inside a metal case. It is difficult to perform electromagnetic simulation for amorphous core loop antennas because of the complicated laminate structure. Therefore, we modeled the amorphous metal core loop antenna as an equivalent bulk structure having anisotropic permeability property that we can simulate. We analyzed the receiving sensitivity of the amorphous antenna by calculating the antenna factor. The receiving sensitivity degrades remarkably when an antenna is inside a metal case. We performed further simulation to investigate eddy current losses that cause deterioration.

key words: magnetic core loop antenna, amorphous metal, LF, magnetic field simulation

1. Introduction

Radio controlled watches that use Low-Frequency standard radio waves have become popular in Japan. By receiving standard radio waves, radio controlled watches can provide precise date and time [1]. As there are two time standard radio stations in Japan, the electric field strength that is theoretically achieved is larger than $50 \text{ dB}\mu\text{V/m}$ in the whole territory. But the field strength becomes so weak inside a reinforced concrete building, so the need to improve the receiving sensitivity of the radio controlled watch as much as possible is important.

To achieve better size and design for radio controlled watches, antenna miniaturization is also needed. But it is difficult to miniaturize a radio controlled watch in the same time as to improve its receiving sensitivity because the antenna size is directly proportional to the receiving sensitivity. Thus, this brought us to the necessity of using electromagnetic field simulation to get an optimal design.

Conventionally, radio controlled watches have their antenna arranged in a resin case or an outside resin band of a metal case. Recently, a built-in antenna inside a full metal case is in demand for quality design. As this leads to an inevitable consequence of shielding effect, the receiving sensitivity becomes worse. This design brings another problem,

that is the type of antenna material to be used for the metal case. A ferrite core loop antenna cannot be used in a metal case because it can easily get broken. An amorphous metal core loop antenna is used for such a model instead. But it is difficult to perform electromagnetic simulation because of its complicated laminate structure.

Reference [2] which has done studies on these antennas expressed measurement results of the inductance and Q-factor for the number of laminated amorphous core. But it did not consider the laminate structure in its simulation of inductance, and there was also no comparison between the simulation results and the measured values.

In addition, available literatures that have examined about the influence of a metal case to the receiving sensitivity of a radio controlled watch are rarely seen. Actually in recent years, radio controlled watches that have a built-in antenna inside a full metal case have been manufactured. But little has been done about the mechanism of the sensitivity degradation because only experimental measures were taken. In that sense, this paper may be the first report to analyze the mechanism about the influence of the metal case in radio controlled watches.

We modeled the amorphous metal core as an equivalent bulk structure having anisotropic characteristics in solving the simulation problem. Then we analyzed the receiving sensitivity of the amorphous antenna by calculating the antenna factor. As for the antenna used in the radio controlled watch, there is little degree of freedom on the shape because it is implemented inside a very narrow space. In such space limitation, the opening angle of an amorphous metal core is an important parameter in relation to the receiving sensitivity. Therefore, we performed simulations to evaluate the most suitable opening angle of the amorphous metal core in order to improve the receiving sensitivity.

The measurement results of the antenna factor of the antenna with a metal case indicate that the miniaturization of the antenna built-in a metal case is very difficult. One of the advantages of antenna simulation that include a metal case is the ability to design the antenna that is suitable for various shape cases efficiently. In the first step, we imported CAD data of a metal case from external designs into the electromagnetic field simulator. Then we proceeded to analyze the characteristics of a fully integrated antenna model.

This paper is organized as follows. In Sect. 2, characteristics of amorphous metal core loop antennas are described. Also, the modeling parameters using the equivalent magnetic circuit are explained. In Sect. 3, we examine the

Manuscript received February 5, 2007.

Manuscript revised April 13, 2007.

[†]The author is with the Advanced Research Laboratory, Hamura R & D Center, CASIO Computer Co., Ltd., Hamura-shi, 205-8555 Japan.

^{††}The authors are with the Graduate School of Science and Technology, Tokyo Institute of Technology, Tokyo, 152-8550 Japan.

a) E-mail: abe@rd.casio.co.jp

DOI: 10.1093/ietele/e90-c.9.1784

influence of a metal case by electromagnetic simulation. Finally, we give our conclusions in Sect. 4.

2. Amorphous Metal Core Loop Antenna

Small receiving antennas for LF standard radio, magnetic core loop antennas are now being widely used. As known, the wavelength of the Low-Frequency region is several kilometers, but the antenna size required for radio controlled watches is extremely smaller than the wavelength. This is one big difference compared with an antenna that is used in the microwave frequency.

Previously, we have evaluated a ferrite core loop antenna [3]. But a ferrite core loop antenna is seldom used for a built-in antenna inside a metal case because it is fragile in terms of its strength. An amorphous metal core loop antenna is a better choice for such a model.

2.1 Structure of an Amorphous Core Loop Antenna

Figure 1 shows a picture of an amorphous core loop antenna module used in radio controlled watches. A coil is wound up to a magnetic core. The length of the antenna we considered is 16 mm, and its number of turns is 1,195. The copper wire, which forms the coil, has a diameter of 0.08 mm, while the magnetic body is covered with a resin mold for reinforcement. In Fig. 1, a flexible printed circuit (FPC) was used to implement tuning capacitors which are connected to the antenna.

Ferrite or amorphous metals are usually used for the magnetic core of the antenna. In recent years, amorphous metal cores are used more than ferrite cores for reliability and strength. A ferrite core loop antenna has a bulk structure so it is easy to process. But it can easily get broken. In contrast, an amorphous core loop antenna has a laminated structure. It is hard to break because of its flexibility, but it is also complex to process. Considering the reliability of a product, the amorphous core loop antenna is more suitable as a built-in antenna inside a metal case.

2.2 Modeling for Simulation

An amorphous metal core loop antenna has very thin films, which are laminated to construct a magnetic core. The thickness of one sheet we considered is $16\mu\text{m}$ and its antenna length is about 16 mm. Figure 2 shows how this amorphous

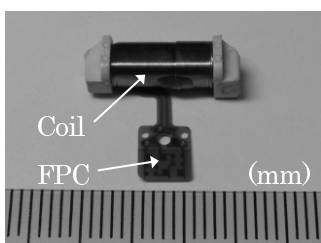


Fig. 1 Amorphous core loop antenna used in radio controlled watches.

laminated structure may look like. Amorphous films are covered with resin mold to keep the strength. To deal with such laminated structure in a finite element electromagnetic simulation is difficult, because the aspect ratio is too large, and accordingly, it demands a huge memory to run. So we modeled the laminated structure by a bulk structure which has the same external shape, but an anisotropic material characteristics.

We derived permeability of the anisotropic material so that the reluctance of the laminated core structure and that of the bulk structure are set equal in each direction. If magnetic flux flows in the magnetic body as shown in Fig. 3, the reluctance of the magnetic body R_m which has a permeability μ , cross-sectional area S , and length ℓ is expressed as

$$R_m = \frac{\ell}{\mu S}. \tag{1}$$

Next, we introduce the toroidal core which has an air gap as a simple model. In Fig. 4, the total reluctance R'_m is considered as a series connection of the reluctance of a magnetic core R_c and air gap R_g [4]. If there is no magnetic flux leakage, the relation between the magnetomotive force and the magnetic flux is expressed as

$$F_m = \phi \left(\frac{\ell - \delta}{\mu_0 \mu_r S} + \frac{\delta}{\mu_0 S} \right) \equiv \phi R'_m, \tag{2}$$

where ℓ is the magnetic path length, μ_0 is the permeability of free space, μ_r is relative permeability of the magnetic body, and R'_m is the total reluctance.

Using the same concept, we apply it to N sheets of magnetic thin films. The reluctance of N pieces of laminated magnetic films can be considered as the reluctance of the magnetic core, which is serially connected with $N - 1$ air gaps. In Fig. 5, we assume the magnetic flux flows along the direction of the Z -axis. The equivalent bulk-structure magnetic body has the same external form, thus the reluctance must be equal. The condition of the Z -component reluctance is written as follows:

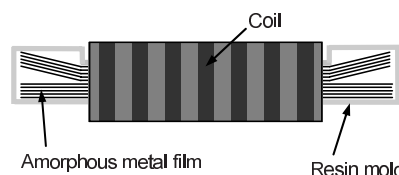


Fig. 2 Structure of an amorphous metal core loop antenna.

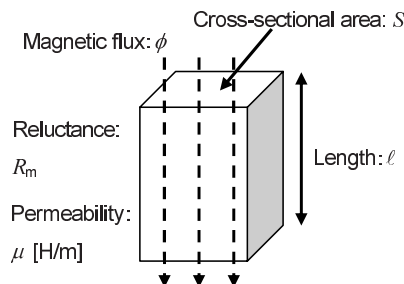


Fig. 3 Reluctance of a magnetic body.

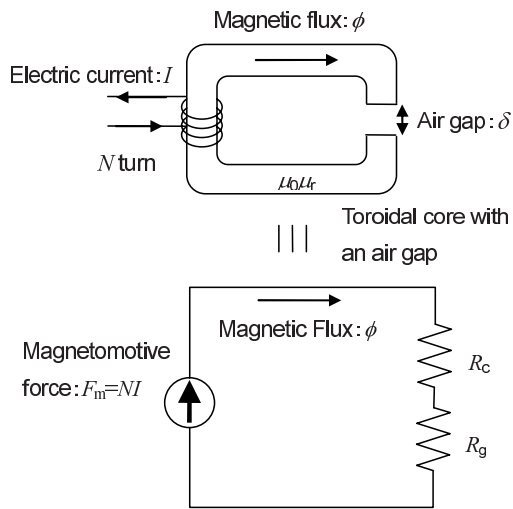


Fig. 4 Toroidal core with an air gap and the equivalent magnetic circuit.

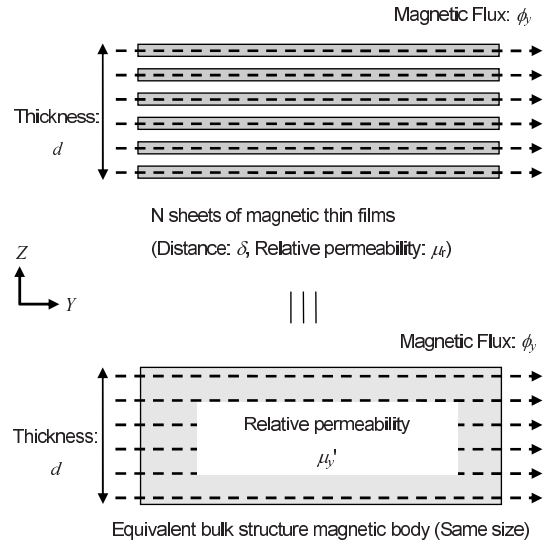


Fig. 6 The magnetic body with the equivalent bulk structure (Y-component).

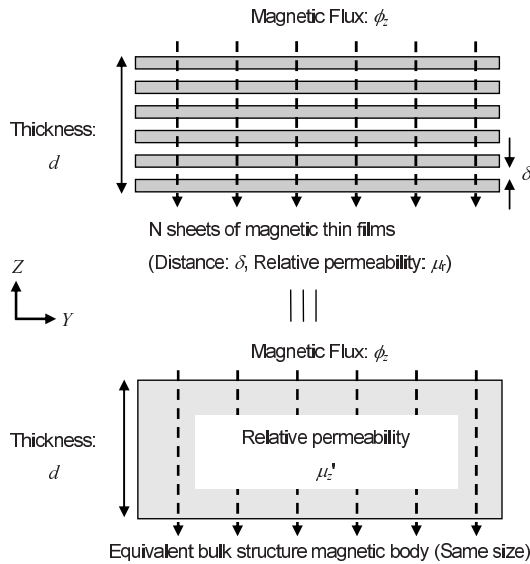


Fig. 5 The magnetic body with the equivalent bulk structure (Z-component).

$$\frac{d - (N - 1)\delta}{\mu_0 \mu_r A} + \frac{(N - 1)\delta}{\mu_0 A} = \frac{d}{\mu_0 \mu'_z A}, \quad (3)$$

where A is the cross-sectional area which a vertically-directed magnetic flux flows into. From Eq.(3), the Z-component relative permeability of the equivalent bulk structure can be written as

$$\mu'_z = \frac{\mu_r d}{d - (N - 1)\delta + \mu_r (N - 1)\delta}. \quad (4)$$

In the same way, we considered the X and Y component permeability of the equivalent bulk-structure model. This time, we assume that the magnetic flux flows in the direction of the Y-axis as shown in Fig. 6. In that condition, the Y-component reluctance of the laminating model is expressed as a parallel connection of the reluctance of N-sheet

magnetic core. Then the reluctance conditions of N sheets of magnetic thin films and the equivalent bulk structure are written as

$$\frac{\ell}{\mu_0 \mu_r \{d - (N - 1)\delta\} w} = \frac{\ell}{\mu_0 \mu'_y w d}, \quad (5)$$

where w and ℓ are the width and length of the magnetic body. There is no dependency on these parameters in Eq. (5), that means it is identical for both X- and Y-components. Then, we can derive the X- and Y- relative permeability components of the equivalent bulk-structure model as follows:

$$\mu'_x = \mu'_y = \frac{d - (N - 1)\delta}{d} \mu_r. \quad (6)$$

In addition, the conductivity of the equivalent bulk magnetic body can be derived in a similar way. The relation of the Y-component electrical resistance of laminating N pieces of magnetic films and that of the equivalent bulk-structure model is expressed as

$$\frac{\ell}{\sigma \{d - (N - 1)\delta\} w} = \frac{\ell}{\sigma'_y d w}, \quad (7)$$

where σ is the conductivity of the magnetic body. From Eq. (7), the X- and Y- conductivity components of the equivalent bulk-structure model is expressed as

$$\sigma'_x = \sigma'_y = \frac{\sigma \{d - (N - 1)\delta\}}{d}. \quad (8)$$

The Z-component conductivity of the equivalent bulk structure is regarded as 0 because each of the magnetic sheet is insulated. The relations of the permeability tensor and the conductivity tensor are expressed as follows:

$$\begin{bmatrix} B_x \\ B_y \\ B_z \end{bmatrix} = \begin{bmatrix} \mu_0 \mu_x & 0 & 0 \\ 0 & \mu_0 \mu_y & 0 \\ 0 & 0 & \mu_0 \mu_z \end{bmatrix} \begin{bmatrix} H_x \\ H_y \\ H_z \end{bmatrix}, \quad (9)$$

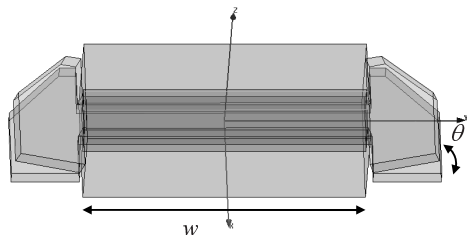


Fig. 7 Simulation model for the amorphous core loop antenna.

Table 1 Relative permeability and calculated anisotropic permeability.

Frequency	μ_r	(μ'_x, μ'_y, μ'_z)
40 kHz	8900	(6675, 6675, 4)
50 kHz	8800	(6600, 6600, 4)
60 kHz	8700	(6525, 6525, 4)

$$\begin{bmatrix} J_x \\ J_y \\ J_z \end{bmatrix} = \begin{bmatrix} \sigma_x & 0 & 0 \\ 0 & \sigma_y & 0 \\ 0 & 0 & \sigma_z \end{bmatrix} \begin{bmatrix} E_x \\ E_y \\ E_z \end{bmatrix}. \quad (10)$$

2.3 Simulation of the Inductance and the Antenna Factor

We performed simulation analyses for an amorphous metal core loop antenna by setting up the equivalent bulk-structure model as mentioned in the previous section. Figure 7 shows the simulation model of the amorphous core loop antenna depicted in Fig. 1. The length of the antenna, the thickness of the antenna, the number of amorphous sheets, the winding width of the coil w , the number of turns N , and opening angle of the amorphous core θ is 16 mm, 4.5 mm, 40, 11 mm, 1195 turn, and 17°, respectively. Table 1 shows the relative permeability of the amorphous core and calculated anisotropic permeability at the operating frequency. As a simulation tool for a small LF antennas, we used ANSOFT Maxwell 3D [5]. It is based on the finite element method (FEM), and is generally used for magnetic field simulation for low frequencies also.

The magnetic core model in Fig. 7 was made as follows: 1) make two rectangular solid which have a thickness of 20 amorphous films each; 2) cut both ends of upper part magnetic core and bend each of them by 17°; 3) unite the upper part of the magnetic cores again; and 4) set the anisotropic material property to upper and lower magnetic cores.

For the simulation condition, we generated an external magnetic field of 40 kHz, with a magnetic strength of 0.839 $\mu\text{A/m}$ that corresponds to an equivalent TEM electric field strength of 50 dB $\mu\text{V/m}$.

First, we investigate the distribution of the magnetic flux density of an antenna magnetic core when it receives the magnetic field. Figure 8 (a) shows the simulation result of the magnetic flux density with the permeability and conductivity set isotropically. It does not seem to show the characteristic of the amorphous core because the magnetic body inside the coil does not have a magnetic flux density difference between the upper surface and side surface. On

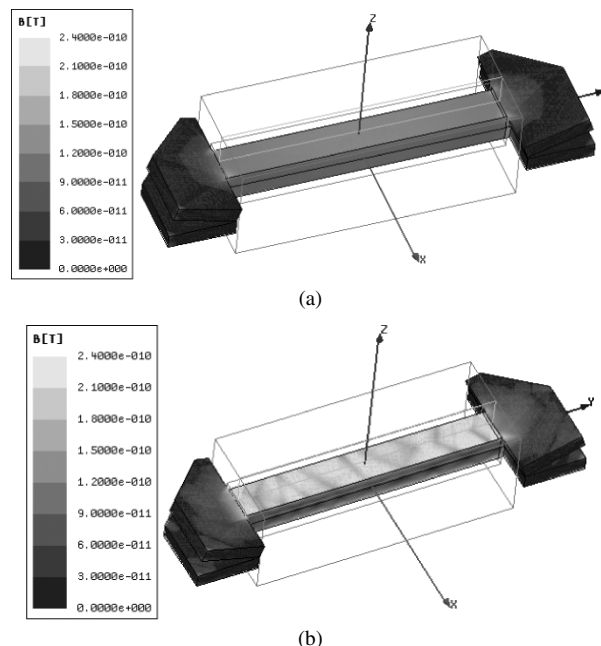


Fig. 8 (a) Magnetic flux density of the isotropic magnetic core. (b) Magnetic flux density of the anisotropic magnetic core.

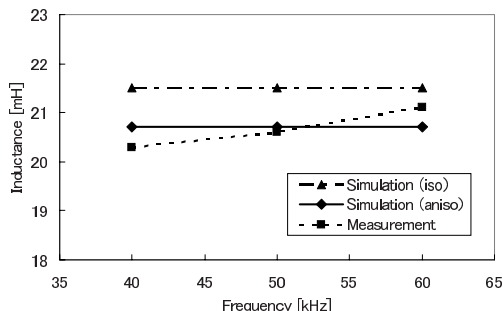


Fig. 9 Simulation result of the inductance.

the other hand, Fig. 8 (b) shows the simulation result setting when the material property was set anisotropically following the equations explained in Sect. 2.2. The amorphous metal core loop antenna has a high magnetic flux density at the surface, while the central part of the side has a low density. This characteristic of this amorphous metal core loop antenna is different from that of the ferrite core loop antenna which has a bulk structure.

As a quantitative evaluation of the magnetic flux feature, we calculated the inductance of the amorphous antenna for both isotropic and anisotropic material properties, and the results compared with the measured values are shown in Fig. 9. The measured values were observed using an impedance analyzer in serial mode. As seen in the figure, the measured inductance becomes larger as frequency increases because of the floating capacitance of the coil. In a low frequency domain less than 40 kHz, the inductance takes almost a constant value of about 20 mH. In the simulation model, the effect of floating capacitance was not considered, so the simulation results with the anisotropic material

were considered to take almost the same measured value. Therefore, the results show that the bulk-structure model with an anisotropic permeability property provides a characteristic of the laminated structure model.

We used the antenna factor to evaluate the receiving sensitivity of the LF antenna. As the impedance is not usually matched between the receiver IC and the antenna in low frequency systems, the antenna factor is an easier and a more realistic parameter than the antenna gain for the LF antenna. The antenna factor AF is defined by the ratio of the electric field strength E at the receiving position to the received voltage V_0 of the antenna as follows:

$$AF[1/m] = \frac{E[V/m]}{V_0[V]}. \quad (11)$$

We measured the antenna factor of the amorphous core loop antenna by using the substitution method [3]. In our measurements, we confirmed the stability of the measurement system. For evaluating the simulation, we obtained the antenna factor by calculating the magnetic flux of the antenna. From Faraday's law, the received voltage of the antenna V is expressed by the magnetic flux linkage ϕ_i , which goes through the antenna coil, is written as

$$V = - \sum_{i=1}^N \frac{d\phi_i}{dt}, \quad (12)$$

where N is number of turns of the antenna coil. The magnetic flux linkage ϕ_i is a function of the magnetic core position, also because the distribution of the magnetic flux strength is not uniform. By using a tuning circuit, the received voltage is multiplied by the Q-factor at the resonant frequency. Thus, the voltage at the tuned frequency is expressed as

$$V_0 = \omega_0 \sum_{i=1}^N \phi_i Q_0 = 2\pi f_0 N \phi_{ave} Q_0, \quad (13)$$

where Q_0 stands for the Q-factor of the resonance circuit, and ϕ_{ave} is the average value of the magnetic flux linkage of the antenna. The Q-factor of the amorphous core loop antenna is normally 60 to 90 at the operating frequency. The average magnetic flux linkage, ϕ_{ave} , of the antenna is obtained by

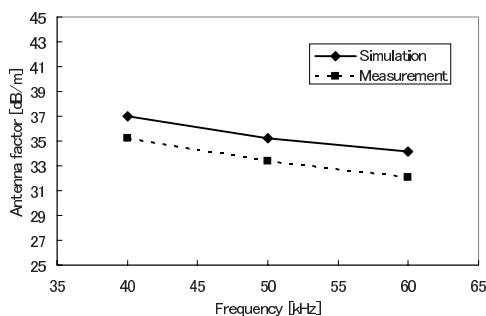


Fig. 10 Simulation result of the antenna factor.

$$\phi_{ave} = \int \left(\iint_{coil} B_y dS \right) dy/w = \iiint_{coil} B_y dv/w, \quad (14)$$

where w is the winding width of the coil.

By calculating Eq. (14) numerically, we obtained the antenna factor of the amorphous metal core loop antenna. Figure 10 shows the simulation results and the measurement values of the antenna factor. The maximum difference between the simulation results and the measurement values of the antenna factor is 2.2 dB. Therefore, our simulation modeling for calculating the antenna factor is reasonably accurate.

2.4 Simulation for Optimized Antenna Design

Looking at the shape of the amorphous metal core in Fig. 2, it is found that both ends of the antenna are V-shaped. The reason for this shape is to improve the receiving sensitivity. To concentrate more magnetic flux, it is effective to widen the cross-sectional area of a magnetic body. But enlarging both ends of the antenna too much will decrease the sensitivity because the length of the magnetic core, for a magnetic field direction, is shortened at the same time.

As for the antenna used for the radio controlled watch, there is little degree of freedom on the shape because it was implemented in a very narrow space. In such space limitation, the opening angle of the both ends of the amorphous core is an important parameter in relation to the receiving sensitivity. Therefore, we performed simulation to evaluate the most suitable opening angle of the amorphous metal core in order to improve the receiving sensitivity.

We calculated the magnetic flux linkage for a given opening angle by magnetic field simulation. Figure 11 defines the opening angle of the amorphous metal core used in the simulation condition. The figure shows only one side of the antenna, but both sides of the antenna have the same opening angle in the actual simulation model. From the simulation results, the behavior of the magnetic flux and inductance is plotted in Fig. 12. The larger magnetic flux linkage means better receiving sensitivity. However, there is no clear relationship between the inductance and the receiving sensitivity. When both sides of the antenna are opened widely, the inductance becomes larger because the magnetic flux forms a closed loop. As a result, an opening angle of 30 degrees gives the maximum receiving sensitivity in our simulation model.

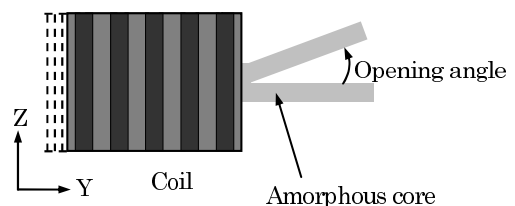


Fig. 11 Opening angle of the amorphous metal core.

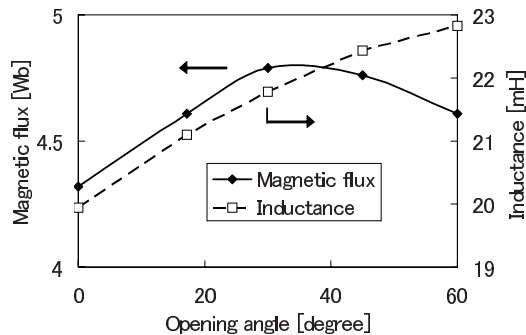


Fig. 12 Magnetic flux and inductance results.



Fig. 13 The interior side of a radio controlled watch with an all-metal casing.

3. Influence of a Metal Case on the Receiving Property of Small LF Antennas

We investigated the influence of a metal case to the characteristics of a magnetic core loop antenna. Eddy current losses were calculated in the fully integrated antenna model.

3.1 Characteristics of the Antenna within a Metal Case

Radio controlled watches which have built-in antennas inside a metal case are highly desired to relatively improve the overall design. However, such an integration causes a degradation of the receiving sensitivity, because the shielding effect and eddy current losses of a metal case are increased. Figure 13 shows the interior side of a radio controlled watch with an all-metal casing. The material of the amorphous metal core of the antenna is the same with that of the antenna shown in Fig. 1, but the length of the antenna is now 21 mm. This slightly longer length is for the compensation of the receiving sensitivity degradation of the antenna built in a metal case. The opening angle of the amorphous core is 17 degrees. It is necessary to consider the influence of a metal case, but the receiving sensitivity may improve by increasing the opening angle of the amorphous core more than that angle as considered in Sect. 2.4.

The external diameter of the metal case considered is about 40 mm and the thickness from the outer case edge to the inner case edge is about 3 mm. For a good conductor, the formula of skin depth is expressed as [6]

$$\delta \approx \sqrt{\frac{2}{\omega\mu\sigma}}, \tag{15}$$

where ω , μ and σ are the angular frequency, permeability, and electrical conductivity, respectively. Figure 14 depicts the calculated skin depth of the stainless steel (SUS316) and titanium casing, using the characteristics of materials given in Table 2. We considered the frequency range from 10 kHz to 80 kHz. Taking into account the penetration of the electromagnetic waves, SUS316 has a better characteristics than titanium. However, radio controlled watches that use a titanium case are preferred in Japan, because titanium is light and allergen-free metal.

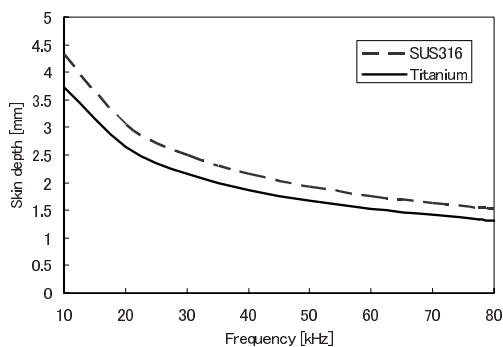


Fig. 14 Skin depth of the metal case.

Table 2 Characteristics of SUS316 and titanium.

	Relative permeability	Conductivity
SUS316	1.01	1.35×10^6
Titanium	1.00018	1.82×10^6

We measured the inductance and the Q-factor of the antenna including the metal case with an impedance analyzer (HP4194A) under a constant room temperature of 25°C. The material of the considered metal case is titanium. The nearest distance between the antenna and the inner case edge is 1.5 mm. That distance has a great influence on the characteristics of the antenna. In Fig. 15, the inductance of the antenna decreased in the case of an antenna-integrated metal case. The frequency dependence of the inductance is related to the stray capacity of the winding. That inductance reduction of the metal case was caused by eddy currents, which flow from the leaking magnetic flux from the antenna, thus weakening the overall magnetic flux of the antenna.

Figure 16 shows the measurement results of the Q-factor. The Q-factor of the antenna becomes about $\sim 1/10$ when the antenna is integrated in the metal case. The Q-factor based on the general definition is expressed by the ratio of the stored energy at a frequency f and the energy loss as follows:

$$Q = \frac{2\pi f W}{P_r + P_1 + P_{case}} \approx \frac{2\pi f W}{P_1 + P_{case}}, \tag{16}$$

where W is the stored energy of the antenna, and P_r , P_1 , and

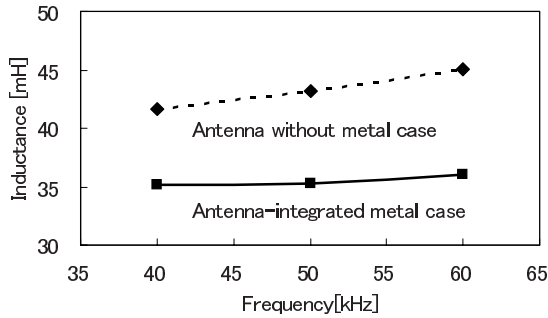


Fig. 15 Measured inductance of the antenna with and without a metal case.

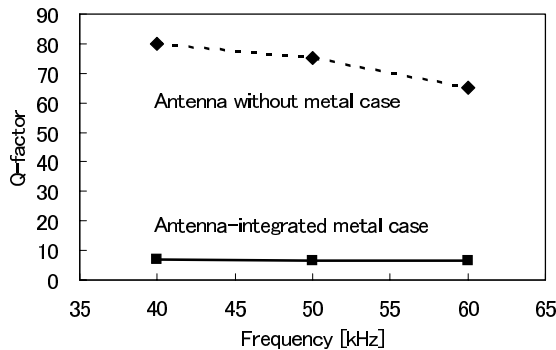


Fig. 16 Measured Q-factor of the antenna with and without a metal case.

P_{case} stand for the radiation energy per unit time, energy loss of the antenna per unit time, and the energy loss of the case per unit time, respectively. The radiation energy P_r can be ignored in comparison with P_l and P_{case} ($P_r \ll P_l, P_{\text{case}}$) because the size of the antenna is extremely smaller than the wavelength. The measured results of Fig. 16 indicate that the energy loss of the case was dominant in Eq. (16). Therefore, to increase the Q-factor, we need to decrease the energy loss of the metal case.

The degradation of the Q-factor has an obvious effect on the receiving sensitivity. Figure 17 shows the measured antenna factor of the antenna with and without a metal case. The measurement results of the antenna factor indicate that the sensitivity degradation with the influence of a metal case was about 23 dB. This means that it is difficult to downsize the antenna built in a metal case. Therefore, simulation analysis including a metal case is necessary to realize antenna miniaturization.

3.2 3D CAD Data Import

To perform the eddy current simulation of the fully-integrated antenna model, we previously inputted the shape dimension of the metal case directly into a magnetic field simulator [7]. But it may be a problem to input a complicated metal-case model into the magnetic field simulator, because we need large amount of time and effort to input a three-dimensional (3D) curved shape precisely. For that reason we used an import method by using a conversion tool which translates the intermediate data to input data for

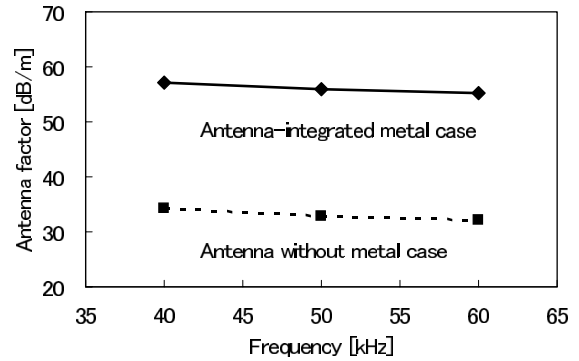


Fig. 17 Measured antenna factor of the antenna with and without a metal case.

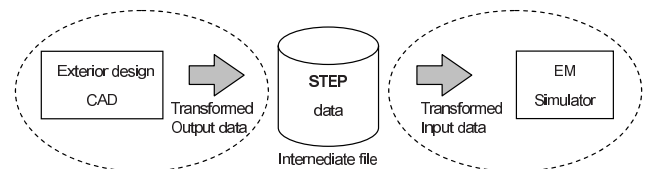


Fig. 18 Importing external CAD data by way of intermediate file.

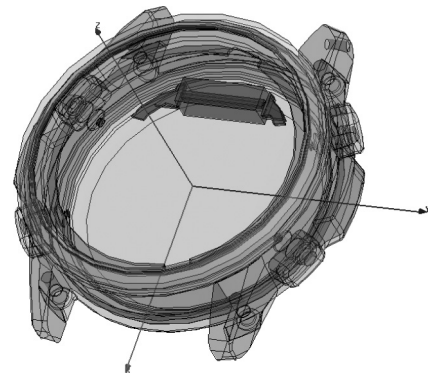


Fig. 19 Simulation model including metal case.

the electromagnetic simulator as shown in Fig. 18. We used STEP (Standard for the Exchange of Product model data) format as the standard intermediate data format. Figure 19 shows the simulation model after importing the 3D-CAD data of the exterior housing design. The shape of the antenna model was inputted directly. The coil part of the antenna was modeled as bulk 1 turn coil which has the thickness equivalent to 1,630 turns and its conductivity was set to that of a copper.

3.3 Using a Metal Case for a Radio Controlled Watch

We investigated eddy currents that are generated in a metal case by simulation. The fully-integrated antenna model was put in a magnetic field of 40 kHz. The 40 kHz magnetic field was generated to the direction of the Y-axis as shown in Fig. 20. The magnetic field strength was set to $0.839 \mu\text{A/m}$, which corresponds to the equivalent TEM electric field strength of $50 \text{ dB}\mu\text{V/m}$.

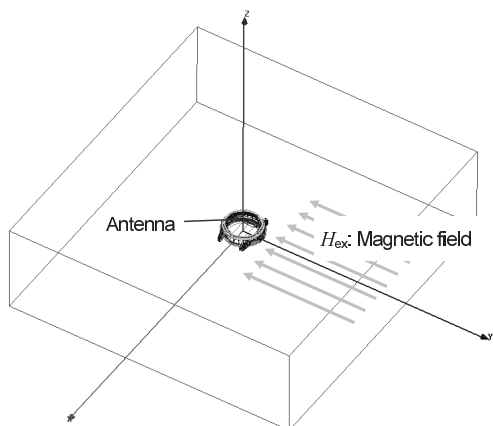


Fig. 20 Simulation area and external magnetic field.

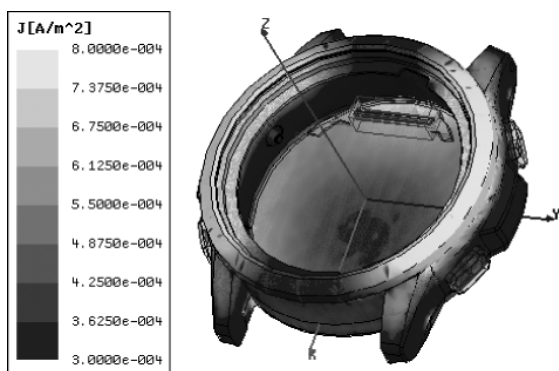


Fig. 21 Eddy currents generated in the metal case.

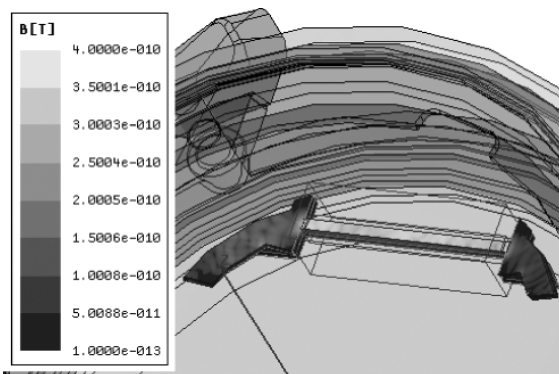


Fig. 22 Magnetic flux density of the amorphous metal core.

The simulation result of the electric current density strength that was generated in the metal case is indicated in Fig. 21. The primary observed result is that eddy currents are stronger near the antenna and at both sides of the bezel. The eddy currents just below the antenna were caused by the magnetic flux that leaked from the coil of the antenna. Figure 22 shows the magnetic flux density of the amorphous metal core inside the case. The magnetic flux linkages become larger inside the coil due to the effect of both sides of the larger magnetic core.

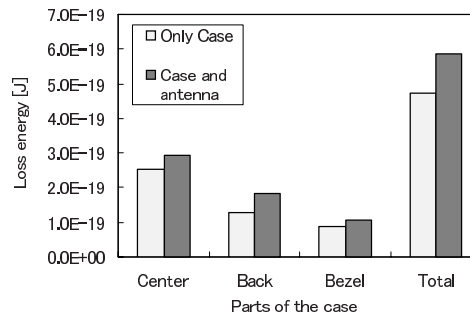


Fig. 23 Energy loss of each part of the case.

3.4 Energy Loss of the Metal Case

We obtained the energy loss of the metal case quantitatively. The heat loss of the eddy currents is expressed as

$$P_{loss} = I_{eff}^2 R = \frac{1}{2} \int_{case} \frac{(\mathbf{J} \cdot \mathbf{J}^*)}{\sigma} dV, \tag{17}$$

where I_{eff} is the effective current that flows through whole metal case, J is the complex current density, and σ is the conductance. We performed eddy current simulations to calculate the integral of the current density amplitude, which is generated at each part of the metal case. Figure 23 shows the calculation results for energy loss, which is compared with and without the antenna inside the metal case. The energy loss of the metal case with an antenna inside is larger because the magnetic flux from the antenna is leaking to the metal case. Especially, the back of the case has the largest eddy current effect from the magnetic flux leakage.

3.5 Magnetic Flux near the Receiving Antenna

We performed magnetic field simulation for the magnetic flux distribution near the receiving antenna. To improve the receiving sensitivity, it is important to know the flow of magnetic flux near the antenna. Figures 24 and 25 show the cutting planes to show the magnetic field vector. The simulation result of the magnetic field looking along the X-axis is shown in Fig. 26. Most of the magnetic field goes from the clockface to the antenna, because the amorphous metal core of the antenna has larger permeability than that of air.

The magnetic field looking along the Z-axis is shown in Fig. 27. The magnetic field from outside the case is shielded, so the magnetic field from inside the clockface is the strong part of the magnetic flux.

To improve the receiving sensitivity, reducing the eddy current loss is necessary as we mentioned in Sect. 3.1. It means we must prevent the magnetic flux leakage from the antenna to the metal case. Keeping the distance between the antenna and the metal case is one of the ways to deal with the problem, despite the limitation of the implementation space. Another way is to change the path of the magnetic flux by arranging a lossless magnetic sheet between the antenna and the metal case.

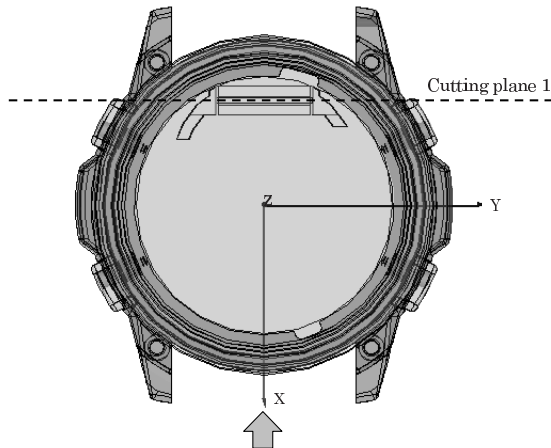


Fig. 24 Cutting plane 1 when looking along the X-axis.

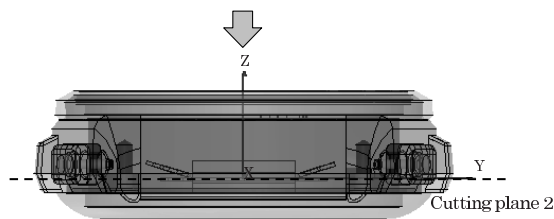


Fig. 25 Cutting plane 2 when looking along the Z-axis.

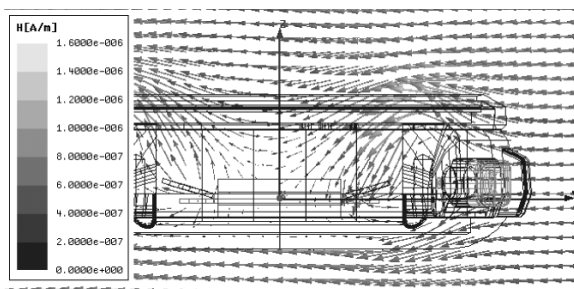


Fig. 26 Magnetic field looking along X-axis.

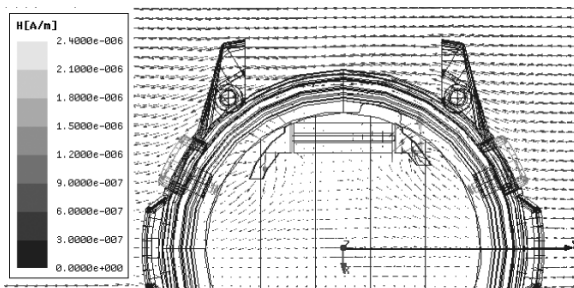


Fig. 27 Magnetic field looking along Z-axis.

4. Conclusion

In this paper, we first discussed a method of evaluating the performance of an amorphous metal core loop antenna that

has a laminated structure. It can be modeled by an equivalent bulk structure that is handled in the simulator by setting it to have anisotropic characteristics. In addition, the simulation results agree with the measurement results. The opening angle of an amorphous metal core is an effective parameter in a limited space. In the model we evaluated, the flux linkage is maximum when the opening angle of the amorphous core is about 30 degrees. In evaluating the fully-integrated antenna model, we found that eddy currents of the metal case were stronger near the antenna and at both side of the bezel. To improve the receiving sensitivity of the antenna, reducing the eddy current loss that is generated in the metal case is necessary. By evaluating the performance of built-in antennas inside a metal case, we can advance to an antenna design that can be adapted to various case shapes.

References

- [1] Japan Standard Time Group, <http://jty.nict.go.jp/>
- [2] H. Iura, M. Asama, Y. Katahara, T. Hamaya, Y. Yamada, K. Watanabe, Y. Iseki, and H. Ishii, "A study on amorphous antenna of radio wave for frequency and time standard," Industrial Research Institute of Niigata Prefecture Research Report, 2005.
- [3] K. Abe and J. Takada, "Simulation and design of a very small magnetic core loop antenna for an LF receiver," IEICE Trans. Commun., vol.E90-B, no.1, pp.122-130, Jan. 2007.
- [4] G.R. Slemmon, *Magnetolectric Devices*, pp.130-133, John Wiley & Sons, USA, 1966.
- [5] Ansoft Corporation, <http://www.ansoft.com/>
- [6] C.A. Balanis, *Advanced Engineering Electromagnetics*, p.150, John Wiley & Sons, USA, 1989.
- [7] K. Abe and J. Takada, "Performance evaluation of a very small magnetic core loop antenna for an LF receiver," Proc. Asia-Pacific Microwave Conference 2006, pp.935-938, TH3C-4, Yokohama, Japan, Dec. 2006.



Kazuaki Abe received the B.S. and M.S. degrees in physics from University of Tsukuba, Tsukuba, Japan, in 1990 and 1992, respectively. He joined CASIO Computer Co., Ltd., Tokyo in 1992. His current research interest is LF antenna for radio controlled watches. He was the recipient of the 2006 Asia-Pacific Microwave Conference APMC Prize.



Jun-ichi Takada received B.E. and D.E. degrees from Tokyo Institute of Technology, Japan, in 1987 and 1992, respectively. From 1992 to 1994, he has been a Research Associate at Chiba University, Chiba, Japan. From 1994 to 2006, he has been an Associate Professor at Tokyo Institute of Technology, Tokyo, Japan. Since 2006, he has been a Professor at Tokyo Institute of Technology. His current research interests are wireless propagation and channel modeling, antennas and antenna systems for wireless

applications, and cognitive radio technology. He is a member of IEEE, ACES, and ECTI Association Thailand.